Neurobiology of Disease

Combination of Thrombin and Matrix Metalloproteinase-9 Exacerbates Neurotoxicity in Cell Culture and Intracerebral Hemorrhage in Mice

Mengzhou Xue,[1] Morley D. Hollenberg,[2] and V. Wee Yong[1]

[1]Hotchkiss Brain Institute and Department of Clinical Neuroscience and [2]Department of Pharmacology and Therapeutics and Department of Medicine, University of Calgary, Calgary, Alberta, Canada T2N 4N1

The rapid loss of neurons is a major pathological outcome of intracerebral hemorrhage (ICH). Several mechanisms may produce the neurotoxicity observed in ICH, and these include proteolytic enzymes such as thrombin and matrix metalloproteinase-9 (MMP-9). We tested the hypothesis that thrombin and MMP-9 combine to injure neurons in culture and that they interact to promote the acute neurotoxicity that occurs in ICH *in vivo*. We report that human fetal neurons die when exposed to thrombin or MMP-9 in isolation and that a combination of these two enzymes increased neurotoxicity. The toxicity of thrombin involved protease-activated receptor-1 and the conversion of proMMP-9 to active MMP-9. In ICH, which was induced in mice by the intracerebral injection of autologous blood, significant areas of brain damage, neuronal death, microglia/macrophage activation, and neutrophil accumulation occurred by 24 h of injury. Importantly, these neuropathological features were reduced in MMP-9 null mice compared with wild-type controls, and the concordant antagonism of thrombin using hirudin also alleviated the injury found in MMP-9 null mice. Our collective results demonstrate that thrombin and MMP-9 collaborate to promote neuronal death in culture and in ICH. To improve the prognosis of ICH, the neurotoxic actions of thrombin and MMP-9 must be inhibited early and simultaneously after injury.

Key words: **thrombin; MMP-9; proteases; inflammation; neuronal death; ICH**

Introduction

Intracerebral hemorrhage (ICH) results from the rupture of cerebral vessels leading to the development of a hematoma in the brain parenchyma. ICH accounts for ~15–20% of all strokes but has a worse prognosis than the predominant form caused by ischemia. Effective medical treatment for ICH has been unsatisfactory (Qureshi et al., 2001), although recombinant-activated Factor VIIa administered within 4 h of ICH was found recently to impair the growth of hematomas and improve functional outcomes (Mayer et al., 2005). Hematomas constitute a significant problem because the blood itself seems to have adverse effects beyond its space-occupying effect (Mendelow, 1993). Detrimental molecules in blood may include proteolytic enzymes, such as thrombin, that are released into the CNS parenchyma (Xue and Del Bigio, 2001).

In vitro, thrombin induces neurite retraction (Yoshida and Shiosaka, 1999) and neuronal apoptosis (Citron et al., 1997), partly through the activation of protease-activated receptors (PARs) (Cocks and Moffatt, 2000). When injected into the brain, thrombin causes brain edema (Lee et al., 1996), perhaps by lysis of vascular basement membrane (Figueroa et al., 1998), which results in neuronal death (Xue and Del Bigio, 2001). The use of hirudin to inhibit thrombin activity, after the injection of blood into rodent brain, reduced brain edema (Lee et al., 1996) and cell death (Xue and Del Bigio, 2005).

Besides thrombin, other proteases may also be important contributors to brain pathology. Particularly, the family of matrix metalloproteinases (MMPs) (Yong et al., 2001) are implicated in stroke injury, including in ICH (Rosenberg and Navratil, 1997; Montaner et al., 2003; Wang and Lo, 2003; Cunningham et al., 2005). The intracerebral injection of bacterial collagenase, which is related to mammalian MMPs, leads to ICH with blood–brain barrier disruption, edema, and tissue necrosis (Rosenberg et al., 1998). ICH caused by bacterial collagenase is associated with an increase in levels of various MMPs (Power et al., 2003), and the pathological consequences are reduced by treatment with inhibitors of metalloproteinases, such as BB-1101, BB-94, and GM6001 (Rosenberg and Navratil, 1997; Lapchak et al., 2000; Wang and Tsirka, 2005). Of the MMP family members, MMP-9 appears to be particularly relevant to ICH in humans (Rosell et al., 2006). Perihematoma edema is closely associated with MMP-9 levels and neurological worsening (Abilleira et al., 2003), as is the probability of hemorrhagic transformation (Castellanos et al., 2003).

Given that both thrombin and MMPs are present concur-

Received March 13, 2006; revised Aug. 9, 2006; accepted Aug. 10, 2006.

This work was supported by a grant from the Canadian Institutes of Health Research (CIHR). V.W.Y. holds the Canada Research Chair in Neuroimmunology. M.X. was supported by fellowships from the CIHR and Alberta Heritage Foundation for Medical Research. We thank Yan Fan, Claudia Silva, and Mahmoud Saifeddine for skilled technical assistance.

Correspondence should be addressed to Dr. V. Wee Yong, University of Calgary, 3330 Hospital Drive, Calgary, Alberta, Canada T2N 4N1. E-mail: vyong@ucalgary.ca.

DOI:10.1523/JNEUROSCI.2806-06.2006

 0270-6474/06/2610281-11$15.00/0

rently in ICH, their combinational roles in mediating neurotoxicity deserve better attention. Here, we have addressed whether thrombin and MMP-9 are neurotoxic *in vitro* and after ICH *in vivo*. Specifically, we addressed whether these proteases interact to mediate the neurotoxicity that occurs within 24 h of ICH. Our results show that both proteases produce the early brain damage after ICH and that they collaborate to exacerbate injury. Targeting both enzymatic systems would be important in alleviating the significant pathology of ICH.

Materials and Methods

Preparation of human fetal neurons and their treatment. Human fetal neurons (HFNs) were used as the targets of neurotoxicity in cell culture as reliable sources of recombinant human MMP-9, whereas human thrombin was obtained commercially. Cells were isolated from the brains of 15–22 week gestational specimens obtained at legal, therapeutic abortions. The use of human fetal cells was approved by the local institutional human ethics committee. The method for obtaining HFNs has been described previously (Vecil et al., 2000). In brief, brain tissue was diced into small fragments and incubated in 0.25% trypsin and 200 μg/ml DNase I in PBS. The suspension was then filtered and centrifuged. The pellet was resuspended in PBS and recentrifuged, and after a final wash in feeding medium, the cells were plated into T75 flasks coated with polyornithine (10 μg/ml). The plating density was 80 million cells in 25 ml of medium. To obtain neuron-enriched cultures, cells in the flasks were treated with at least three cycles of 25 μM cytosine arabinoside (2 d on, 3 d off) to kill dividing astrocytes. The feeding medium during this time was minimum essential medium supplemented with 10% fetal bovine serum, nonessential amino acids, 1 mM sodium pyruvate, 2 mM glutamine, and 10% dextrose. All culture medium supplies were from Invitrogen (Burlington, Ontario, Canada). The resulting cells after three cycles of cytosine arabinoside treatment were neurons in excess of 90% purity, with astrocytes, microglia, and precursor cells forming the rest. The neuron-enriched cultures, henceforth called HFNs, were retrypsinized and plated at 100,000 cells/well in 16-well Lab-tek slides (Nunc, Naperville, IL) in the above medium.

Thirty minutes before an experiment, the serum-containing medium was switched to a serum-free AIM-V medium (Invitrogen), so that any proteases or factors present within serum would not confound the interpretation of results. Test enzymes or vehicle controls were then applied. Thrombin (from human plasma, T4393; Sigma, St. Louis, MO) was used at final concentrations of 1–10 U/ml, whereas active recombinant human MMP-9 (83 kDa; Calbiochem, La Jolla, CA) was used at final concentrations of 50–200 ng/ml.

In experiments in which inhibitors were used, these inhibitors were added 30 min before MMP-9 or thrombin. To inhibit MMP-9, we used an MMP-9 inhibitor (100 ng/ml; Calbiochem) or the broad-spectrum metalloproteinase inhibitors BB94 (500 nM; British Biotech, Oxford, UK) and GM6001 (5 μg/ml; Calbiochem). The potent and selective antagonist of human PAR-1, SCH79797 [*N*3-cyclopropyl-7-[[4-(1-methylethyl)phenyl]methyl]-7*H*-pyrrolo[3,2-f]quinazoline-1,3-diamine] (Tocris Bioscience, Ellisville, MO) (Ahn et al., 2000), was used to block PAR-1 activity.

Assessment of neuronal death in culture. After 48 h of treatment with proteases, neurons were fixed with 4% paraformaldehyde, washed with PBS, and incubated with mouse anti-human microtubule-associated protein-2 (MAP-2) antibody (1:2000; Sigma) for 1 h to label neurons. A goat anti-mouse Ig conjugated to Cy3 (1:300; Caltag Laboratories, Burlingame, CA) was then applied for 1 h. Hoechst dye (1:100, nuclear yellow; Sigma) was applied for 10 min to label all nuclei, and slides were glass coverslipped with a mounting medium, gelvatol (Vecil et al., 2000). Using an immunofluorescence microscope, designated fields of each well were evaluated in a blinded manner for the number of remaining neurons. The loss of neurons in test slides compared with controls was thus taken as a manifestation of neurotoxicity.

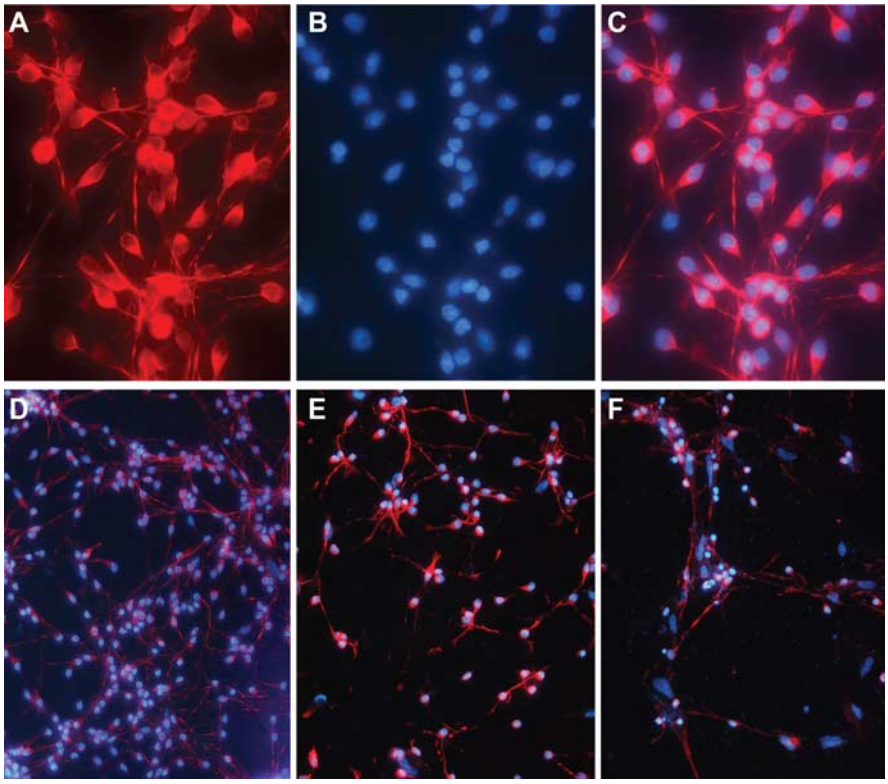

Figure 1. Micrographs of human neurons show their susceptibility to MMP-9 and thrombin toxicity. ***A–C***, High-magnification corresponding views of control neurons labeled for MAP-2 (***A***) and Hoechst dye (***B***), and their overlay (***C***), displaying the high purity of neurons. ***D–F***, Lower-magnification micrographs (red, MAP-2; blue, Hoechst) of a control culture (***D***), cells treated with 2 U/ml thrombin (***E***), or cells treated with 100 ng/ml active-form MMP-9 (***F***).

Production of ICH in mice and their treatment. Although several animal models of ICH are available to address the potential neurotoxicity of proteases, we chose that inflicted by autologous blood to better mimic the sudden deposition of blood in the brain parenchyma after the rupture of vessels in humans (Xue and Del Bigio, 2003). Mice were used in this study to take advantage of the availability of MMP-9 null mice. To produce ICH, 10 μl of autologous blood obtained from the tail was injected into the mouse striatum; preliminary experiments had shown that larger volumes of saline in the mouse striatum evoked significant tissue reaction so that the impact of blood could not be reliably assessed beyond the mass effect.

Mice were anesthetized using a mixture of ketamine/xylazine. Animals were placed in a stereotaxic frame using modified ear-bars fitted with blunt rubber ends designed for mice. Procedures for induction of ICH by autologous blood were modified from the previous studies in rat (Xue and Del Bigio, 2000) and mice (Xue and Del Bigio, 2005). A midline scalp incision was made, and a hole was drilled in the right skull (2.5 mm lateral to midline, 0.02 mm anterior to coronal suture). The animal's tail was then immersed in warm water for 2 min and cleaned quickly with 70% ethanol, and the tip of the tail was then cut. Blood (10 μl) was collected into a needleless sterile insulin syringe without any anti-coagulant. A 26-gauge needle was quickly attached to the syringe and stereotaxically introduced into the striatum 4.5 mm below the surface of the drilled hole in the skull. The 10 μl of blood was injected over 3 min, and the needle

was left in place for another 3 min to minimize backflow. The syringe was then removed slowly. The burr hole in the skull was sealed with bone wax, the scalp was sutured, and the animals were placed in a cage with *ad libitum* access to food and water. Control mice received 10 μl of saline. Because the focus of our study was the acute neurotoxicity in ICH, animals were killed 24 h after the injury for analyses. All experimental procedures were done in accordance with guidelines of the Canadian Council on Animal Care. Protocols were approved by the local experimental ethics committee.

MMP-9 null and background-matched wild-type (129/SvEv) adult (7–8 weeks old) mice were used for this study. The MMP-9 null mice were originally obtained from Dr. Zena Werb (University of California, San Francisco, CA) (Vu et al., 1998) and were bred in-house. Treatment groups included the intracerebral injection of 10 μl of saline as controls, or those that received intracerebral injections 10 μl of autologous blood to produce ICH. To inhibit the thrombin activity that is present in blood, groups of mice were also given intracerebral injections with 10 μl of autologous blood mixed with an additional 2 μl of hirudin (containing 4 U from leech, H7016; Sigma) or saline.

In another series of experiments, blood from MMP-9 null mice were injected into the brain of wild-type animals, whereas blood from wild-type mice were injected into the brain of MMP-9 null animals; these experiments were designed to discriminate between MMP-9 contributed by blood versus that contributed by the brain in mediating ICH. Finally, thrombin (2 U in 1 μl, or 4 U in 2 μl) or an equivolume of saline was injected into the striatum of wild-type and MMP-9 null mice to evaluate the neurotoxicity of thrombin *in vivo*.

Assessment of histopathology in vivo. Mice were overdosed with ketamine/xylazine at 24 h after ICH and were perfused through the heart with ice-cold 10% formalin. The brains were removed and stored in the same fixative for 1–5 d. Fixed brains were cut coronally ~2–3 mm on either side of the lesion center, which were identifiable on the brain surface (see Fig. 6*A*). These blocks were dehydrated and embedded in paraffin. Sections (6 μm) were cut from the rostral to the caudal portion of the damaged brain areas; consecutive sections from three levels 200 μm apart (see Fig. 6*A*) were collected, and a variety of histological and histochemical stains were performed. Routine hematoxylin and eosin staining was used to evaluate brain damage area. Using ImagePro software (Cybernetics, Silver Spring, MD), the damaged area of each section was traced and tabulated. Damaged brain areas were defined by the presence of blood, tissue rarefaction, or necrosis (see Fig. 5*B*). These analyses were evaluated blind by an experienced investigator to minimize observation bias.

Fluoro-Jade staining was used to reveal dying neurons (Schmued et al., 1997) by incubating and gently shaking sections in 0.06% potassium permanganate for 15 min. Fluoro-Jade (0.001%; Histo-Chem, Jefferson, AR) staining solution was applied for 30 min, followed by a PBS wash, drying, and coverslip application. At high magnification (40× objective magnification), and aided by using an ocular reticule, Fluoro-Jade-positive neurons were counted in four fields immediately adjacent to the needle injection/damage site (see Fig. 7*A*), as described previously (Xue and Del Bigio, 2005). Areas with large blood vessels were avoided. Counts were made near the edge of the lesion because the lesion cores should be devoid of viable cells.

Leder (naphthol AS-D chloroacetate esterase; Sigma) stain was used to show granulocyte (neutrophil) infiltration (Xue and Del Bigio, 2000). Granulocyte lysosomes contain a rather specific hydrolase that uses naphthol AS-D chloroacetate as a substrate. The liberated naphthol reacts with the diazonium salt Fast Red Violet LB [5-chloro-4-benzamido-2-methylbenzenediazonium chloride hemi(zinc chloride)] forming red depots. Neutrophils were visualized with Leder stain and counterstained with hematoxylin, and the numbers of positively stained cells displaying multilobed nuclei were counted in a similar manner as described above for Fluoro-Jade. An observer blinded to the experimental protocol did the counting.

Immunohistochemistry using anti-ionized calcium-binding adapter molecule 1 (Iba1) antibody was used to label microglia/macrophages (Wells et al., 2003). Briefly, sections were rehydrated and rinsed with PBS, followed by antigen retrieval using 10 mM sodium citrate buffer, pH

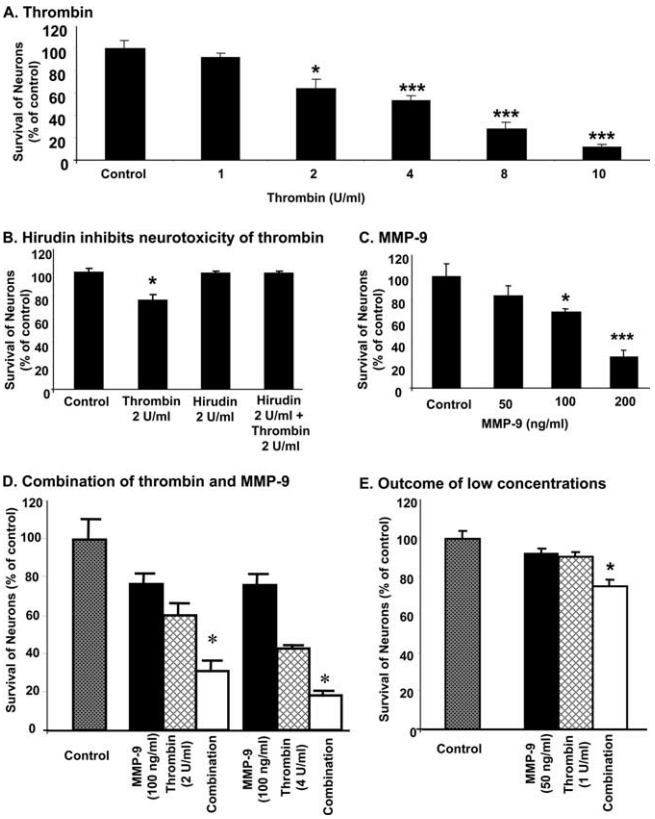

Figure 2. Thrombin and MMP-9 kill cultured neurons in isolation and in combination. The number of neurons remaining in defined fields of a 16-well Lab-tek slide is expressed as a percentage of that in control cultures. ***A***, The concentration effect of thrombin. ***B***, The neurotoxic effect of thrombin is attenuated by a thrombin antagonist, hirudin. Hirudin by itself has no effect on neuronal death. ***C***, The toxicity of active MMP-9 is displayed. $*p < 0.05$, $***p < 0.001$ compared with controls. ***D***, Neurons were treated with active MMP-9 or thrombin at neurotoxic concentrations; the combination of proteases at these concentrations further promoted neuronal death. ***E***, The combination of non-neurotoxic concentrations of thrombin and MMP-9 resulted in cell death. Error bars in ***D*** and ***E*** are statistically different ($p < 0.001$) from the control, and we display only the statistical comparisons between the experimental groups ($*p < 0.001$ compared with either thrombin or MMP-9 alone). Error bars are mean ± SD of four wells, and the trend of the results has been reproduced three times.

6.5. Primary antibody (Millipore, Bedford, MA) was diluted 1:500 and applied to sections overnight at 4°C. Biotinylated anti-rabbit IgG were used as the secondary antibody, and staining was visualized with ABC (Vector Laboratories, Burlingame, CA), using diaminobenzidine as a substrate. Sections were analyzed blind for the degree of microglial/macrophage activation through determination of the morphology and density of the Iba1-labeled cells as described previously (Larsen et al., 2003). Normal resting or quiescent microglia exhibit a distinct morphology, with many ramified processes projecting from the cell body. When activated, these processes begin to retract and thicken, and the microglia take on a more ameboid, macrophage-like appearance. Because markers, including Iba1, cannot differentiate between microglia and macrophages, they are usually referred to microglia/macrophages. Iba1-stained sections were scored for microglia/macrophage activation using a scale of 1–4, in which score 1 was of the least reactivity and score 4 was with the most reactivity of highly activated microglia/macrophages (Wells et al., 2003). Considerations were made for the size, shape, and relative density of Iba1-labeled cells.

In situ *zymography and gel gelatin zymography*. To localize net gelatinolytic activity of MMPs by *in situ* zymography, FITC-labeled DQ-gelatin (available in a gelatinase/collagenase assay kit from EnzChek; Invitrogen, Eugene, OR) was used as a substrate for degradation by gelatinases as described previously (Oh et al., 1999). In its intact form, the FITC of the DQ-gelatin is intramolecularly quenched, but after proteol-

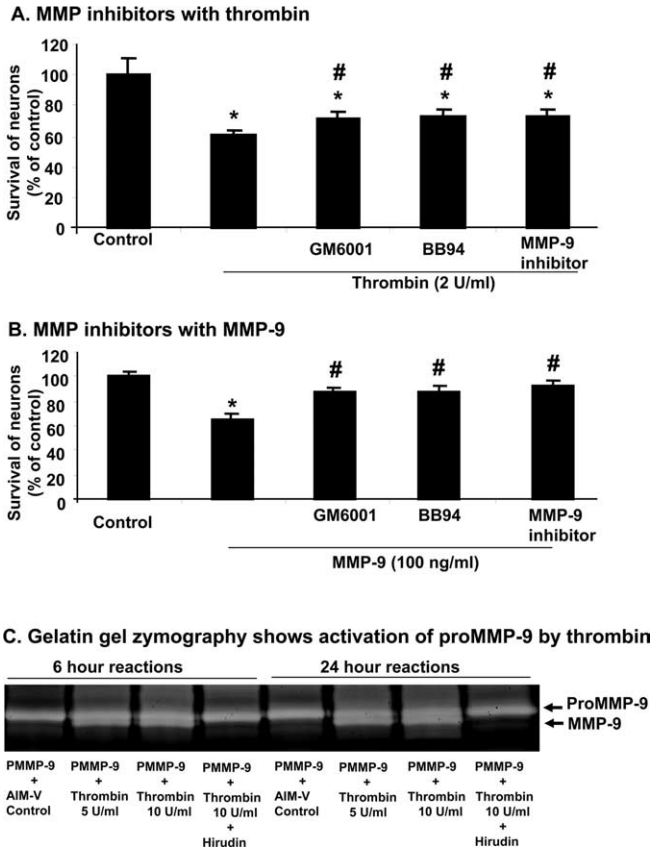

Figure 3. The toxicity of thrombin involves, in part, MMP-9 activation. ***A***, ***B***, Cultured HFNs were treated with MMP inhibitors (5 μg/ml GM6001, 500 nM BB94, and 100 ng/ml MMP-9 inhibitor), and then thrombin was added. The loss of neurons caused by thrombin was reduced by the MMP inhibitors ($^{\#}p < 0.05$ compared with thrombin-treated neurons) but not completely ($p > 0.05$ compared with control). That the MMP inhibitors were used at optimal concentrations is indicated by their reversal of the neurotoxicity of active MMP-9 ($^{\#}p < 0.05$ compared with MMP-9-treated neurons alone; $^{*}p < 0.05$ compared with control). Experiments were reproduced across three sets of cultures with similar results. Error bars indicate SD. ***C***, Zymography shows that some proMMP-9 (PMMP-9) was converted to active MMP-9 (lower band) by thrombin compared with control (the AIM-V cell culture medium was added in place of thrombin), and the specificity of this reaction was confirmed by the absence of conversion when the thrombin antagonist hirudin was present.

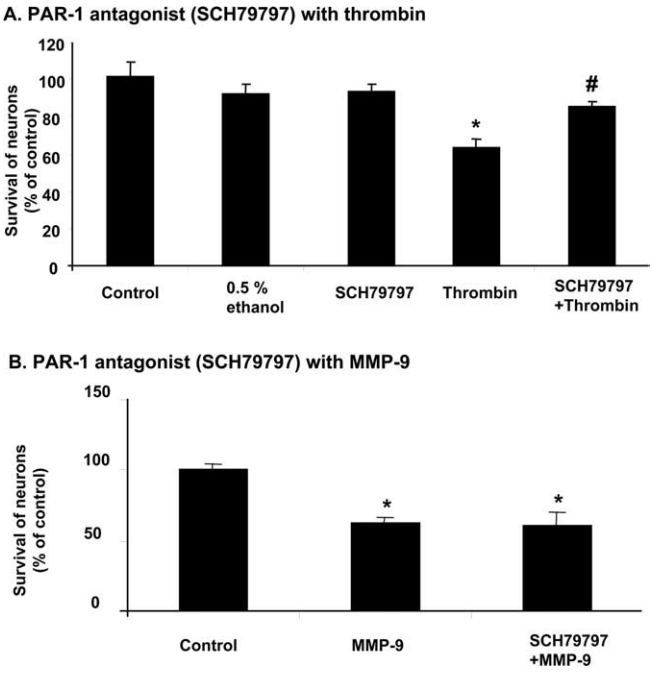

Figure 4. The neurotoxicity of thrombin, but not MMP-9, involves PAR-1 activation. ***A***, The susceptibility of cultured HFNs to thrombin (2 U/ml) was prevented by the PAR-1 antagonist SCH79797 (10 nM). ***B***, In contrast, the PAR-1 antagonist did not affect the toxicity of active MMP-9. Values are mean ± SD of four wells, and the results have been reproduced two times. $^{*}p < 0.05$ compared with control; $^{\#}p < 0.05$ compared with thrombin.

ysis by gelatinases, fluorescence is emitted. The localization of fluorescence indicates the sites of net gelatinolytic activity. Intact and damaged brains at 6 and 24 h after blood injections were removed, dissected on dry ice, quick-frozen with cold isopentane, and stored in −80°C until used. The brain blocks were cut into 14 μm sections using a cryostat (Leica, Wetzler, Germany) and collected sequentially. Sections were thawed and incubated with reaction buffer (0.05 M Tris-HCl, 0.15 M NaCl, 5 mM $CaCl_2$, and 0.2 mM NaN_3, pH 7.6) containing 40 μg/ml DQ gelatin for 3 h. At the end of the incubation period and without fixation or washes, gelatinolytic activity of MMPs was localized and photographed by fluorescence microscopy. Images were acquired by a Spot digital camera.

To measure the amount of MMP-2 and MMP-9, brain blocks of ~2 × 2 × 2 mm^3 size, including the hematoma and adjacent brain tissue (1 mm on either side of the lesion), were taken 24 h after blood injection. Tissues were frozen in dry ice, and MMP-9 protein was extracted using gelatin-Sepharose 4B (Amersham Biosciences, Piscataway, NJ), as described previously (Citron et al., 1997). Briefly, after homogenization of brain tissue in a buffer containing 10 mM $CaCl_2$ and 2.5% Triton X-100, the homogenates were centrifuged at 12,000 × *g* for 30 min at 4°C. The supernatant was recovered and incubated with gelatin-Sepharose 4B for 1 h. The gelatin-Sepharose pellet was resuspended in 100 μl of elution buffer (containing 10% DMSO). The sample was mixed with 4× gel loading buffer (total, 120 μl) and electrophoresed in a 10% SDS gel containing 1 mg/ml gelatin. The gel was incubated in rinse buffer (2.5% Triton X-100, 50 mM Tris, and 5 mM $CaCl_2$) for 6 h at room temperature to remove SDS and to allow renaturation of MMPs in the gel. The gel was then placed in incubation buffer (50 mM Tris, 5 mM $CaCl_2$, and 2 μM $ZnCl_2$) for 48 h to facilitate gelatin degradation by gelatinase. The gel was incubated in Coomassie blue stain solution for 4 h and destained with 10% isopropanol and 10% acetic acid. The areas of gelatinase activity were observed as clear bands against a dark background. The locations of pro- and active-MMP-2 and MMP-9 were based on molecular weight determinations and confirmed by previous experiments (Oh et al., 1999).

To determine whether thrombin can activate proMMP-9 to MMP-9, proMMP-9 (92 kDa, 10 ng; Calbiochem) was diluted in AIM-V medium (total volume, 40 μl; the final MMP-9 concentration was 250 ng/ml); this served as the control. Experimental groups were proMMP-9 (10 ng) mixed with thrombin (final concentrations of 5 and 10 U/ml, respectively) in a volume finalized at 40 μl with AIM-V. A fourth group consisted of the preincubation of hirudin (10 U/ml) with thrombin (10 U/ml) for 30 min, followed by the addition of proMMP-9 (250 ng/ml). Those two sets of four groups were incubated for either 6 or 24 h at 37°C. The sample solutions were then mixed with 4× gel loading buffer and electrophoresed in a 10% SDS gel containing 1 mg/ml gelatin for gel zymography.

Calcium signaling experiments. The interaction of thrombin with PAR-1, a G-protein-coupled receptor, leads to the generation of a calcium signal (Kawabata et al., 1999). To assess the selectivity of the PAR-1 antagonist (SCH79797) for thrombin, calcium signaling experiments were performed. Human neurons were first detached from their adherent substrate using EDTA and suspended in 1 ml of DMEM containing 10% fetal bovine serum. The calcium indicator, fluo-3 acetoxymethyl ester (25 μg/ml), was then added for 20 min at room temperature. After washing to remove excess dye and suspension in buffer (150 mM NaCl, 1.5 mM $CaCl_2$, 20 mM HEPES, 10 mM glucose, and 0.25 mM sulfinpyrazone), fluorescence measurements monitoring elevations of intracellular calcium were conducted at room temperature using a PerkinElmer (Wellesley, MA) fluorometer, with excitation and emission wavelengths of 480 and 530 nm, respectively (Kawabata et al., 1999). Because the aim of this series of experiments was to assess the antagonism by SCH79797 of

thrombin acting via PAR-1, baseline readings were first obtained for thrombin, TFLLR-NH_2 (a selective PAR-1 agonist), and trypsin (a PAR-2 agonist) (Kawabata et al., 1999). SCH79797 was then applied, and the ensuing signals generated by the agonists were re-evaluated.

Statistical analysis. All data are expressed as mean ± SD. Intergroup comparisons were made by ANOVA, followed by Bonferroni's test. The differences were considered significant when $p < 0.05$. We used Graph Pad (San Diego, CA) InStat software for statistical analyses.

Results

Thrombin and MMP-9 kill cultured neurons in isolation and in combination

To take advantage of recombinant MMP-9 and thrombin that are present in the human form, enriched HFNs of >90% purity were used. Figure 1*A–D* is a representative micrograph of cultures, where the majority, if not all, Hoechst-positive nuclei corresponded with MAP-2-positive neurons, and this emphasizes the high purity of the human neurons. When thrombin was applied to HFNs, manifestation of toxicity (reduced number of cells remaining in culture) was already apparent by 24 h and became more pronounced at 48 h. To reduce ambiguity of cell counting, in that a dying/dead cell after 24 h of treatment might not yet have been detached from the coverslip and thus could be tabulated as a MAP-2-positive cell, we evaluated cell density only after 48 h of treatment. We found that thrombin was neurotoxic at 2 U/ml and that higher concentrations produced more death (Figs. 1*E*, 2*A*). MMP-9 also reduced neuronal survival, and this manifested from 100 ng/ml and was readily apparent at 200 ng/ml (Figs. 1*F*, 2*C*).

Recently, some commercial thrombin preparations were found to contain impurities that were responsible for the presumed thrombin effect (Hanisch et al., 2004; Weinstein et al., 2005). Thus, to obviate the possibility that impurities were actually responsible for the neurotoxic action of the thrombin preparation, we incubated neurons with hirudin, a thrombin antagonist, before thrombin application. If an impurity was responsible for the effect of thrombin, then hirudin should not be effective in blocking neurotoxicity. Figure 2*B* shows that hirudin completely reversed the neurotoxicity of thrombin, thereby implicating thrombin rather than impurities in the observed effect.

We next addressed whether there was a combinational effect of thrombin and MMP-9 on toxicity to HFNs. Figure 2*D* shows that the combination of thrombin at concentrations of 2 and 4 U/ml, together with MMP-9 (100 ng/ml), resulted in a significantly greater decrease in neuronal survival compared with either alone. Remarkably, the combination of thrombin and MMP-9 at concentrations that were not neurotoxic in isolation led to the death of neurons (Fig. 2*E*).

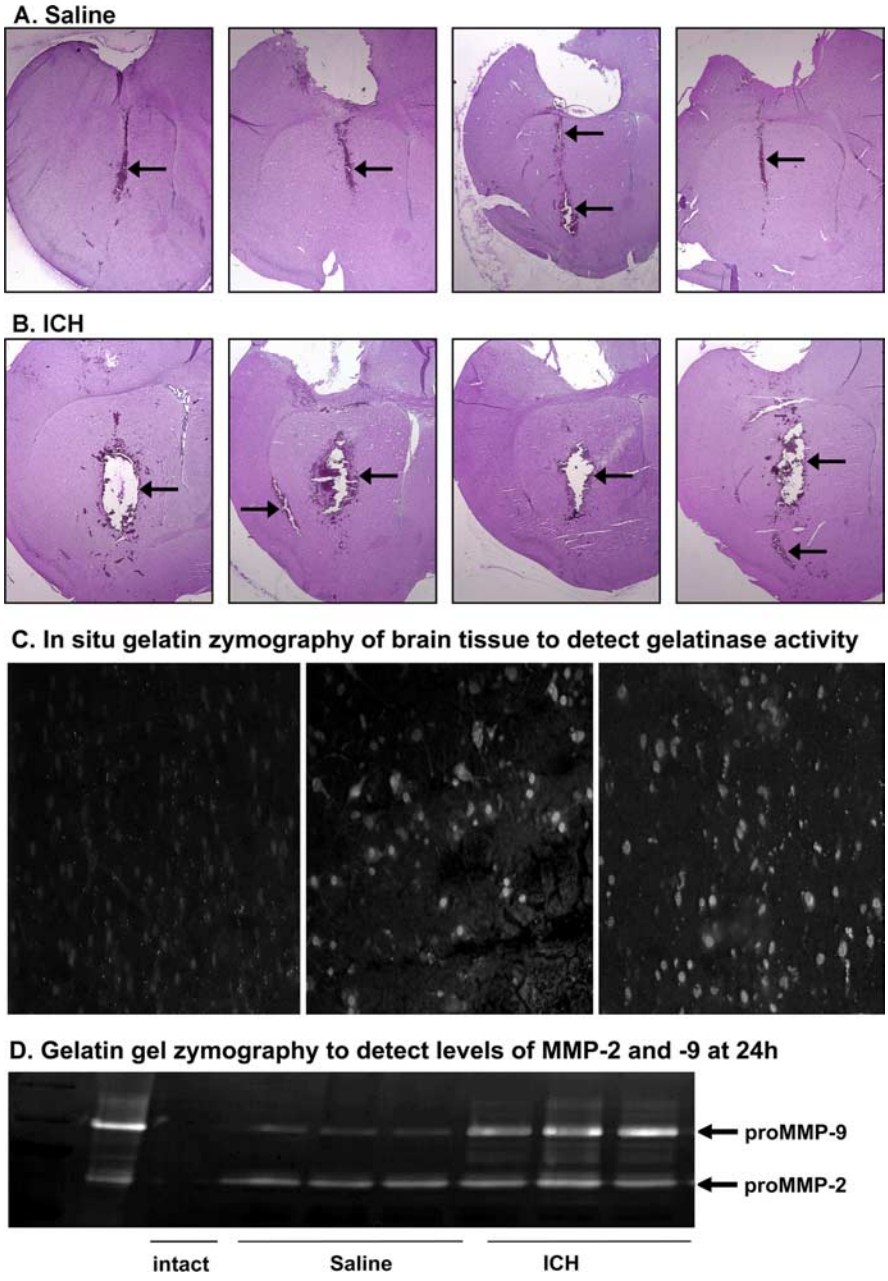

Figure 5. The injection of autologous blood into the right striatum of mice produces injury within 24 h, and this is accompanied by elevations of MMP-9. ***A***, ***B***, Hematoxylin and eosin staining shows that 10 μl of saline (***A***) produces some degree of injury (arrow) in the right striatum, but the same volume of blood (***B***) results in extensive damage (arrow). Representative sections from four different saline-treated mice (***A***) or four blood-induced ICH animals (***B***) are displayed. The indentation of the cortex was caused by the bone wax that was used to seal the burr hole. ***C***, *In situ* zymography reveals that in the uninjured striatum (left), there was negligible gelatinase activity, but this was significantly increased at 6 h (middle) and 24 h (right) after ICH. Activity was on cellular profiles. The areas displayed are immediately adjacent to the border of the hematoma. ***D***, Gel zymography was used to specifically measure the content of the gelatinases MMP-2 and MMP-9. Although the intact striatum had low to negligible MMP-2 and MMP-9 expression in the condition examined, this was upregulated in the striatum of saline-treated mice and was increased further in striatal samples of ICH mice. Each lane represents homogenate from individual mice. The extreme left lane contains proMMP-2 and proMMP-9 standards.

The mechanism of thrombin neurotoxicity involves MMP-9 and PAR-1

We evaluated the mechanisms by which thrombin is neurotoxic and addressed specifically whether this involves MMP-9. Cultured

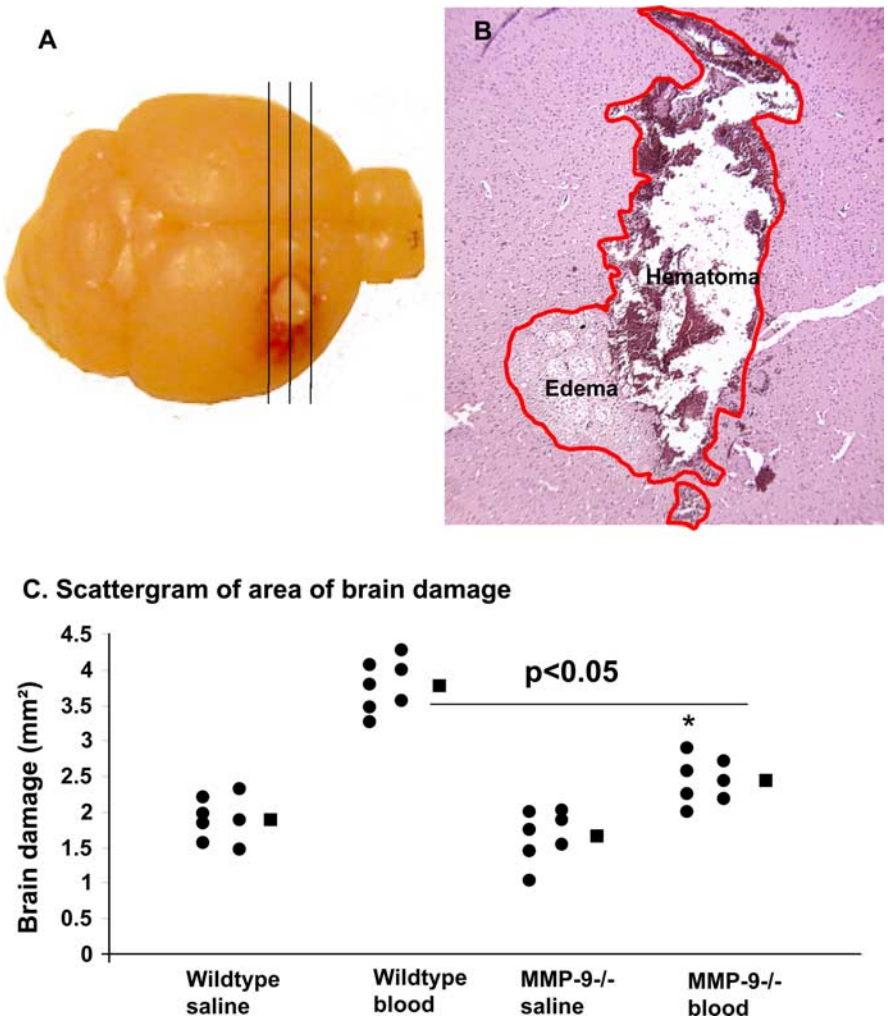

Figure 6. ICH in MMP-9 null mice is less damaging than that in wild-type animals. ***A***, The brain from a wild-type ICH mouse was processed for evaluation, and the three lines represent the three coronal levels taken for histology. Brains from MMP-9 null mice had less discernible global pathology, but the three coronal sections were also taken at similar levels to that displayed here for the wild-type animals, so that similar areas of the brain were sampled in all mice. ***B***, The damaged striatum 24 h after autologous blood injection includes hematoma, necrosis, and edema. ***C***, The area of brain damage from the three sections of each mouse is added and is represented as an individual circle. The square box depicts the mean of the seven mice in each group. The groups were either wild-type or MMP-9 null mice given intracerebral injections of 10 μl of saline or blood. *$p < 0.05$ compared with wild-type mice given injections of blood.

HFNs were pretreated for 30 min with metalloproteinase inhibitors, and thrombin was then added. Figure 3*A* shows that the toxicity of thrombin was partially, but not completely, reversed by GM6001 and BB94. A role for MMP-9 in the mechanism of thrombin toxicity was confirmed by the ability of the MMP-9 inhibitor to partially abrogate the thrombin effect. That these inhibitors were used at optimal concentrations is supported by the control result that the three inhibitors all completely reversed the toxicity of MMP-9 on HFNs (Fig. 3*B*). These results indicate that the neurotoxicity of thrombin involves MMP-9 activity, but other mechanisms are also operative.

To elucidate how the neurotoxicity of thrombin involves MMP-9, we addressed whether thrombin could activate MMP-9 from its pro-form. Figure 3*C* shows that the incubation of proMMP-9 with thrombin resulted in the appearance of the active form of MMP-9, and this was blocked by the presence of hirudin. Thus, the interaction of thrombin and MMP-9 involves, in part, the activation of MMP-9.

To determine additional mechanisms of thrombin neurotoxicity, and given that thrombin is known to activate PAR-1, HFNs were treated with 0.5% ethanol (vehicle solution) and a PAR-1 antagonist, SCH79797, for 30 min, and then thrombin was applied. Figure 4*A* shows that although thrombin reduced neuronal numbers, this effect was abrogated, albeit incompletely, by the PAR-1 antagonist. In contrast, the PAR-1 antagonist did not reduce the neurotoxicity of MMP-9. These data indicate that the neurotoxicity of thrombin, but not MMP-9, involves PAR-1 activation.

To further evaluate the activity of SCH79797, calcium signaling experiments in neurons were performed. We determined that SCH79797 selectively blocked the elevation of intracellular calcium in neurons produced by thrombin and another PAR-1 agonist, TFLLR, but that SCH79797, a selective PAR-1 antagonist, did not alter the effect of the PAR-2 agonist, trypsin (supplemental Fig. 1, available at www.jneurosci.org as supplemental material). These results strengthen the contention that thrombin can act on neurons through a PAR-1-dependent mechanism.

In summary, the tissue culture experiments reveal that thrombin and MMP-9 kill neurons and that their combination further increases the likelihood of death. The mechanisms of thrombin neurotoxicity involve, in part, MMP-9 activity and PAR-1. We sought, then, to investigate the role of these proteases *in vivo* in the context of acute neurotoxicity in ICH.

ICH induced by autologous blood in mice and the increase in MMP-9 level

Mice tolerated the injection of autologous blood into the striatum well. There was no mortality, no seizures, and no apparent deficits in locomotion. Nonetheless, at 24 h after autologous blood injection, a large area of injury (Fig. 5*B*) was readily discernible in the striatum, and there was edema, blood debris, inflammatory cells, and necrosis. In contrast, control mice given an injection of an equivolume amount of saline displayed only a minimal collection of blood, damaged brain, and negligible edema around the needle tract (Fig. 5*A*).

With respect to other histological features of autologous blood-induced ICH at 24 h, we detected the presence of neutrophils, activated microglia/macrophages, and dying neurons. These will be discussed below when comparing between responses in wild-type and null mice.

The regional and cellular localization of gelatinase activity in the brain of wild-type mice subjected to ICH was studied by incubating tissue sections with a masked fluorescent-tagged gelatin substrate. In regions or cells where gelatinolytic activity was present, fluorescence would be observed. The activity of MMP-9 and MMP-2 could not be distinguished by this method because they are both gelatinases. In the intact striatum, only background

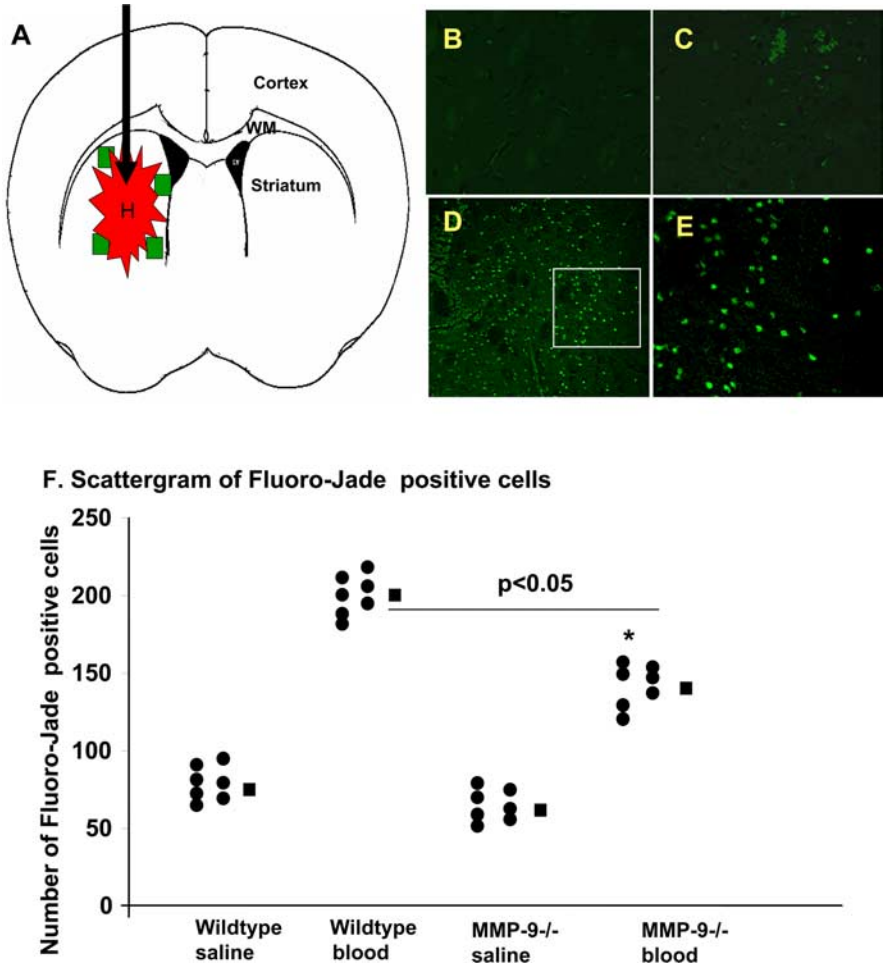

Figure 7. Fluoro-Jade staining was used to detect dying neurons. ***A***, The schematic diagram shows the four areas (green squares) around the hematoma (H) that were counted for Fluoro-Jade-positve cells. WM, White matter. ***B–D***, Fluoro-Jade staining shows no dying neurons detected in normal brains (***B***), a small increase in dying neurons in saline-injected mice (***C***), and an elevated quantity in blood-injected mice (***D***). ***E***, Higher magnification of the boxed area illustrated in ***D***. ***F***, Blinded quantitative analysis of Fluoro-Jade staining (summing the counts obtained at the 3 coronal levels described in Fig. 7) reveals that although blood increases the number of dying neurons compared with saline in wild-type mice, blood in MMP-9 null mice produced a decreased number of dying neurons (*$p < 0.05$ between wild-type and MMP-9 null mice). Values from individual mice are depicted as circles, and the mean of each group is presented as a square.

fluorescence was observed (Fig. 5*C*, left). At 6 h of ICH, there were numerous discrete cells with overlying fluorescence (Fig. 5*C*, middle) confined to the area of injury, and this increased further at 24 h (Fig. 5*C*, right). Thus, gelatinolytic activity indicative of MMP-2 and MMP-9 is increased in ICH around the site of injury.

To measure specifically the elevated level of MMP-2 or MMP-9, gelatin gel zymography was performed. This is an enzyme-based assay dependent on the ability of MMP-2 and MMP-9 to degrade the gelatin substrate impregnated into gels. Figure 5*D* shows that a control striatum has minimal amounts of MMP-2 and MMP-9 in the conditions assayed and that both saline and blood injections elevated MMP-2 and MMP-9 levels. However, brains with ICH had even more expression of MMP-9 compared with saline injections.

In summary, ICH injury produces necrosis, hematoma, and other histological changes in the striatum within 24 h. Concurrent with this, the MMP-9 level and activity are elevated.

ICH in MMP-9 null mice is less damaging than that in wild-type animals

To ascertain the role of MMP-9 in the acute neurotoxicity after ICH, we injected autologous blood into wild-type or MMP-9 null mice and assessed the histopathology 24 h later. Using sections from three specified regions of the brain (Fig. 6*A*), and tracing the areas of brain damage by virtue of their containing necrosis, hematoma, and edema (Fig. 6*B*), seven mice per group were evaluated blind at 24 h of ICH injury.

Saline injection into wild-type or MMP-9 null brains resulted in minor brain damage, and this was not significant between groups. The injection of blood into wild-type brain resulted in significant brain damage. However, the same volume of autologous blood into MMP-9 null mice resulted in less brain-damaged areas (Fig. 6*C*) compared with those in wild type.

Similarly, the quantitative data of Fluoro-Jade-positive dying neurons (Fig. 7) and neutrophil infiltration (Fig. 8) demonstrates that the result of ICH injury was significantly reduced in MMP-9 null mice compared with wild-type animals. In this regard, the sum number of Fluoro-Jade-positive dying neurons or neutrophils in the three levels of brain lesion was significantly increased after intracerebral injection of autologous blood compared with an equivolume amount of saline in wild-type and MMP-9 null mice (Figs. 7, 8). However, the number of Fluoro-Jade-positive dying neurons and neutrophils was significantly reduced after ICH in MMP-9 null mice compared with wild-type controls.

In the vicinity of brain injuries, MMP-9 elevation is the result of that brought in by blood and leukocytes, as well as that produced by neural cells (Yong et al., 2001). To evaluate whether the toxicity of MMP-9 in ICH is as a result of particular sources, we injected 10 μl of blood from wild-type mice into a MMP-9 null brain, or blood from MMP-9 null mice into a wild-type brain. We noted no difference in the size of brain damage or number of dying neurons between the two groups (supplemental Fig. 2, available at www.jneurosci.org as supplemental material), thus indicating that MMP-9 from blood and brain played equivalent roles in mediating the pathology of ICH.

Microglia activation and macrophage migration into the CNS are common occurrences in CNS trauma; we used Iba1 immunoreactivity to address the status of these mononuclear phagocytes in ICH. Analyses of intact uninjured brains revealed that the number of Iba1-positive cells was comparable between wild-type and MMP-9 null mice (Fig. 9*A*,*D*). The sum scores of microglia/macrophage reaction, as evident by the increased density of Iba1-stained cells and by their more ameboid morphology, were significantly increased after intracerebral injection of autologous blood in both wild-type and MMP-9 null mice compared with

saline treatment (Fig. 9*B*,*C*,*E*,*F*). Significantly, comparisons of ICH injury between wild-type and null mice show the microglia/macrophage reaction was decreased in MMP-9 null mice compared with wild type (Fig. 9*G*).

In summary, ICH elicits a diminished neuropathological response in animals genetically deficient for MMP-9, consistent with a role of MMP-9 in mediating neurotoxicity in ICH.

Collaboration of thrombin and MMP-9 in ICH injury

The injection of thrombin into the brain has been reported to produce brain damage (Lee et al., 1996, 1997; Xue and Del Bigio, 2001, 2005). We first addressed whether thrombin toxicity would involve MMP-9 *in vivo* by injecting thrombin into the striatum of wild-type or MMP-9 null mice. The intracerebral injection of 2 μl of thrombin caused significant brain damage (Fig. 10*A*) and Fluoro-Jade-positive cells (Fig. 10*B*) in wild-type mice. However, these indices were reduced in MMP-9 null mice, thus indicating that thrombin neurotoxicity *in vivo* is modulated, in part, by MMP-9.

We next investigated the involvement and collaboration of MMP-9 and thrombin in ICH. Comparison between wild-type and MMP-9 null brains 24 h after ICH reveals a smaller brain-damaged area and a lower number of dying neurons in MMP-9 null animals (Fig. 10*C*,*D*), confirming previous results (Figs. 6, 7) that a mechanism of neurotoxicity of blood involves MMP-9. To probe the role of thrombin, hirudin was administered in the blood that was deposited into the striatum of mice. In both wild-type and MMP-9 null brains, the neurotoxicity of ICH was reduced by hirudin, denoting that thrombin activity in blood facilitated injury in ICH. Significantly, a smaller brain-damaged area and dying neurons occur in mice with both MMP-9 deficiency and hirudin treatment, compared with all other groups. These results emphasize that the mode of toxicity in ICH involves the combination of thrombin and MMP-9.

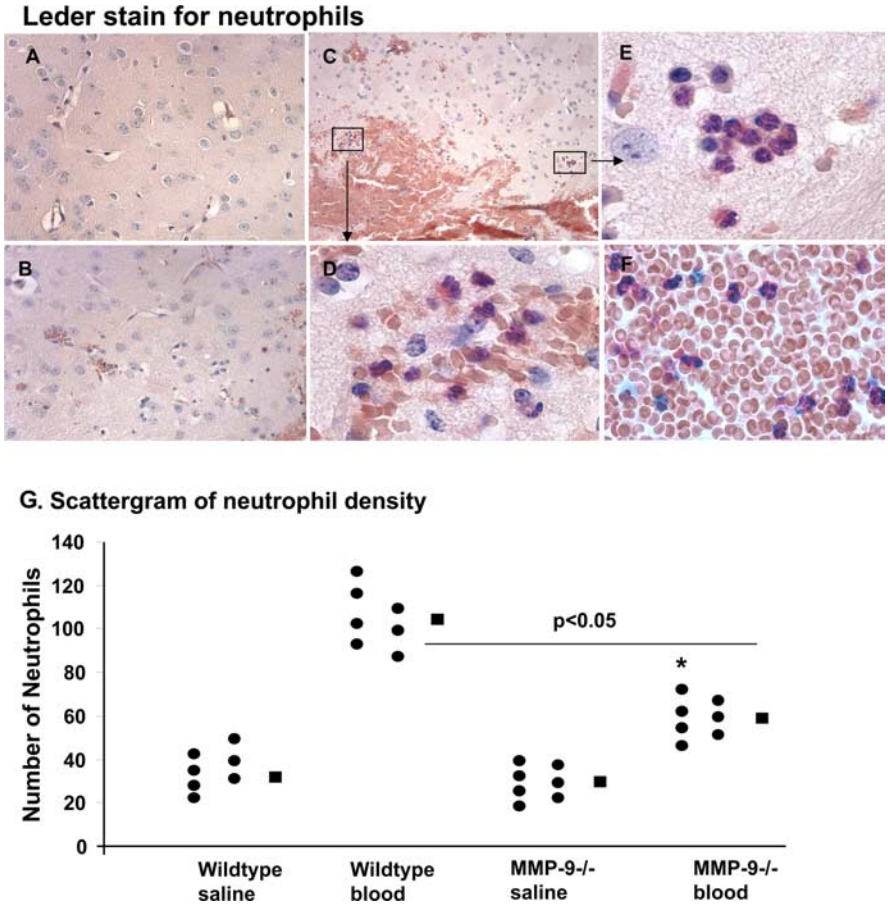

Figure 8. Neutrophil infiltration 24 h after ICH is less in MMP-9 null mice than in wild-type animals. Neutrophils were detected by Leder stain and were counted in the striatum adjacent to the injury site (see Fig. 7*A*, green squares). ***A–C***, There were no detectable neutrophils in normal brains (***A***), a small number in saline animals (***B***), and a significantly elevated count in blood-injected mice (***C***; low-magnification view). ***D***, ***E***, High-magnification views of the boxes in ***C***. ***F***, Neutrophils within the hematoma. ***G***, Blinded analysis reveals a lower number of neutrophils in MMP-9 null mice compared with wild type when injected with blood (*$p < 0.05$). Values from individual mice are depicted as circles, and the mean is presented as a square.

Discussion

ICH causes brain damage through various pathways including inflammation-related mechanisms, local ischemia, and the release of toxins and proteolytic enzymes (Aronowski and Hall, 2005; Xi et al., 2006). With respect to proteases, both thrombin and MMPs have been implicated in brain injury after ICH. We confirm here that thrombin is harmful in culture and show that its injection into the striatum of mice produces neurotoxicity within 24 h (Fig. 10).

We considered whether the concentrations of thrombin we used were within achievable ranges *in vivo*. Because thrombin at injury sites would be derived from prothrombin, we noted that the concentration of prothrombin that is present in plasma is between 260 and 360 U/ml (Colman et al., 1994; Berne and Levy, 1998). Because plasma is ~60% of the volume of blood, the concentration of prothrombin in whole blood would thus be between 430 and 600 U/ml. Thus, if only a fraction (e.g., 1%) of prothrombin were converted to thrombin in ICH, this would result in 4.3–6 U/ml thrombin being available, which is in the range at which we found thrombin to be neurotoxic (Fig. 2) and at which thrombin can maximally activate PAR-1 (Kawabata et al., 1999). A caveat is that we do not know precisely where thrombin would be distributed in ICH, either trapped in the center of the hematoma or available at the spreading margin. These considerations are important in view of the possibility that thrombin at 0.01 U/ml is neuroprotective in culture, whereas 10 U/ml is neurotoxic (Striggow et al., 2000)

MMPs have also received attention as contributors to damage produced by ICH (Rosenberg, 2002; Wang and Tsirka, 2005). Various MMPs of the 24 MMP member family are potential contributors to cell death in ICH, because multiple ones are upregulated in neural injury; in ICH caused by the intracerebral injection of bacterial collagenase, we found MMP-3, -12, and -14 elevated among nine MMPs addressed (Wells et al., 2005). Indeed, we did not find MMP-9 transcripts to be increased in the acute period of collagenase-induced ICH in mice (Wells et al., 2005), but this did not negate the importance of this protease because a significant load of preformed MMP-9 is deposited in-

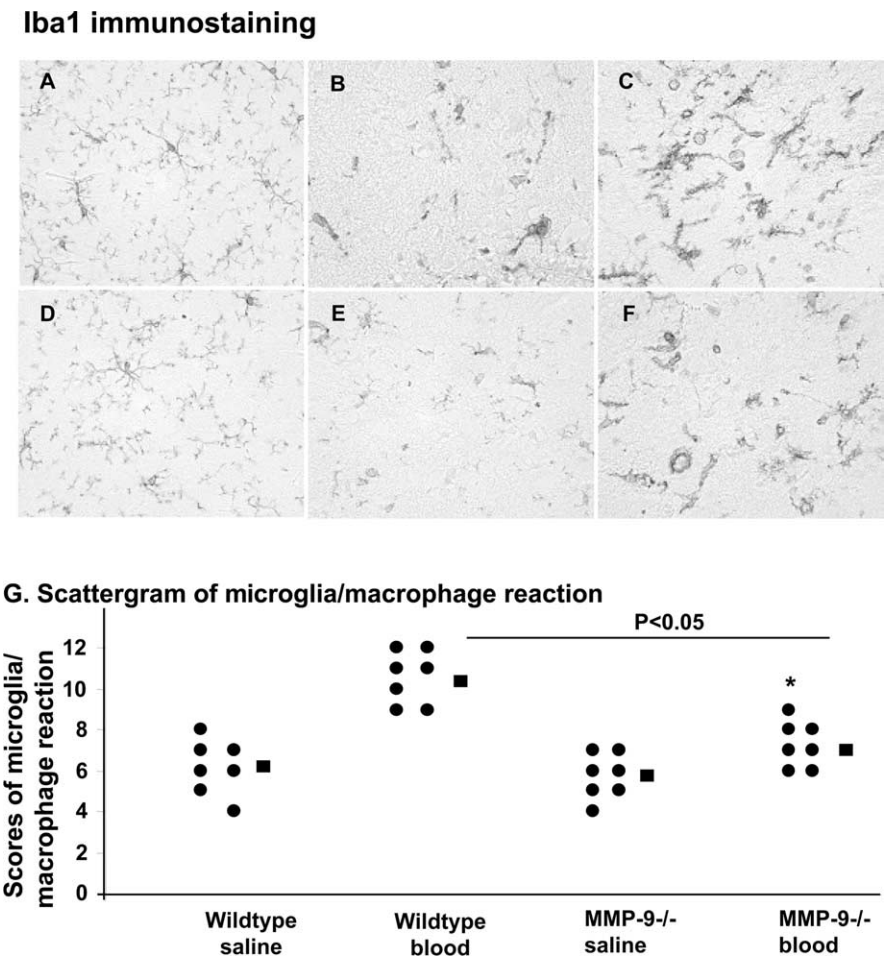

Figure 9. Microglia/macrophage reaction is reduced in MMP-9 null mice after ICH. ***A***, ***D***, Representative sections from normal wild-type and MMP-9 mice, respectively; they demonstrate that there is no obvious differences in microglia in the normal uninjured brain tissue. ***B***, ***E***, After injury with saline, the ramified microglia transforms to ameboid morphology with fewer processes (***B***, wild type; ***E***, MMP-9 null mice). ***C***, ***F***, With blood injection, a greater degree of microglia activation is seen in wild-type (***C***) compared with MMP-9 null (***F***) mice. ***G***, Blinded analysis of the sum scores of microglia/macrophage reaction reveals higher activation in wild-type compared with MMP-9 null mice (*$p < 0.05$). Values from individual mice are depicted as circles, and the mean is presented as a square.

tracerebrally by the neutrophils that come into injured tissue (Opdenakker et al., 2001; Yong, 2005).

In human ICH injury, of the many MMP family members, MMP-9 appears to be particularly relevant (Rosell et al., 2006). Perihematoma edema is closely associated with MMP-9 levels and neurological worsening (Abilleira et al., 2003), as is the probability of hemorrhagic transformation (Castellanos et al., 2003).

Although thrombin and MMP-9 are implicated separately in ICH, their collaboration in mediating neurotoxicity remains to be addressed. In considering first the *in vivo* model to use, we chose ICH induced by autologous blood to better simulate the sudden exposure of the normal brain parenchyma to a hematoma. In contrast, ICH induced by the intracerebral injection of bacterial collagenase generates first a microglia reaction before the enzyme-mediated disruption of the basement membrane leaks blood into the parenchyma. In analyzing the autologous blood-induced ICH model, we note that the injection of 10 μl of whole blood into the mouse striatum is associated at 24 h with brain damage, neuronal death, and inflammation. Besides the toxicity of the deposited blood, the 10 μl volume could alter CNS hemodynamics and physiological blood flow during the course of the experiments. We do not know whether hemodynamics and blood flow were affected, but our controls had included mice given injections of an equivolume amount of saline.

Using the autologous blood-induced ICH model, we determined that tissue injury was less severe in MMP-9 null mice compared with wild-type controls, establishing the involvement of MMP-9 in the significant death of neurons within the first 24 h of ICH injury. The involvement of thrombin in ICH injury is supported by the result that thrombin was neurotoxic when injected intracerebrally and that the detriment of autologous blood was alleviated by the inclusion, in blood, of a thrombin antagonist, hirudin. Significantly, the use of hirudin in MMP-9 null mice, representing the simultaneous antagonism of both MMP-9 and thrombin, resulted in the least degree of brain damage and other histological outcomes, emphasizing the collaboration of both proteases in autologous blood-induced ICH.

It can be argued that the neurotoxicity of MMP-9 or thrombin *in vivo* occurs through indirect mechanisms. In this regard, because MMPs are involved in leukocyte infiltration into the damaged CNS (Yong et al., 2001), the reduced infiltration of neutrophils into the ICH injury site (Fig. 8), and concordant decrease in neutrophil-derived toxins, would be an indirect means by which MMP-9 deficiency resulted in lowered neurotoxicity. Alternately, because MMP-9 interacts with nitric oxide to generate a toxic intermediate (Gu et al., 2002), the lack of this intermediate in MMP-9 null mice could be another manner in which the loss of MMP-9 reduced neurotoxicity. Although these indirect mechanisms of MMP-9 toxicity could be operative in ICH, we demonstrate here that MMP-9 can, in fact, kill neurons when added to cells in culture. It is likely that a combination of direct neurotoxicity of MMP-9 and the indirect mechanisms discussed is responsible for the loss of neurons within 24 h of ICH.

As with MMP-9, thrombin could be killing neurons in ICH through a variety of mechanisms. Because broad-spectrum MMP inhibitors only partially reversed the neurotoxicity induced by thrombin, but yet completely blocked MMP-9-dependent cell death (Fig. 3), suggests that the residual toxicity observed with thrombin is mediated through an MMP-independent pathway. We envisage a direct cytotoxic effect of thrombin through PAR-1 activation, as well as an indirect mechanism through the activation of MMP-9, as our cell culture experiments would suggest (Fig. 4). Importantly, the combination of thrombin and MMP-9 in killing neurons could be demonstrated *in vitro* as well as *in vivo*. We note that reports of the interaction of thrombin and MMP-9 can be found in the published literature, but this involves the increase in MMP-9 transcripts or protein by thrombin (Liu et al., 2000; Stephenson et al., 2005). MMPs are produced as proforms and require activation by autocatalysis or cleavage by other proteases (Yong et al., 2001; Rosenberg, 2002). Our demonstra-

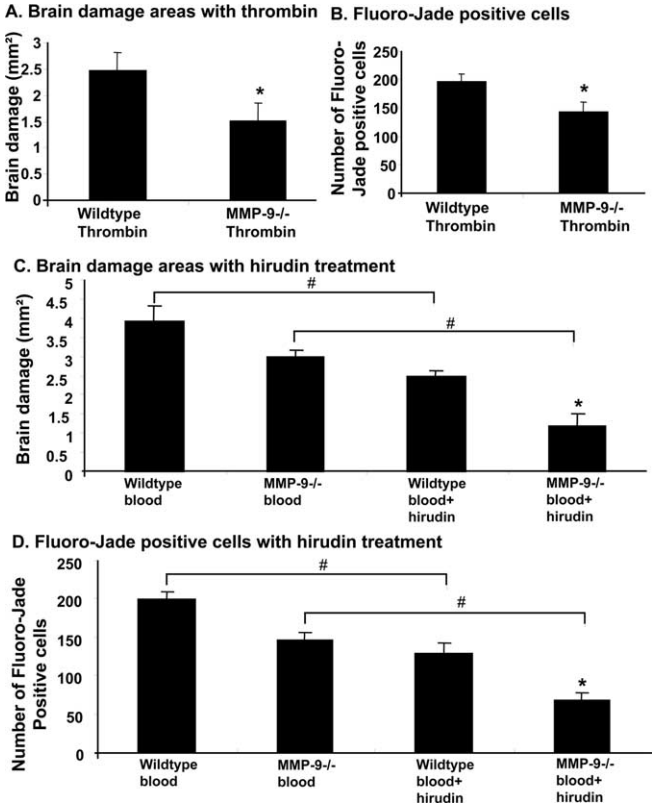

Figure 10. The combination of thrombin and MMP-9 promotes injury in ICH. ***A***, ***B***, The consequence of thrombin (4 U in 2 μl) was first assessed by injection into the striatum of wild-type or MMP-9 null mice. The sum of the brain-damaged area (***A***; $^{*}p < 0.05$) and Fluoro-Jade-positive neurons (***B***; $^{*}p < 0.05$) was significantly reduced in MMP-9 null mice compared with wild-type mice after thrombin. ***C***, ***D***, The effect of ICH was assessed in wild-type or MMP-9 null mice in the presence of thrombin blockade with hirudin. The area of brain damage (***C***) and number of Fluoro-Jade-positive neurons (***D***) was least in MMP-9 null mice treated with hirudin compared with all other groups ($^{*}p < 0.001$). $^{\#}p < 0.001$ when comparing between the subsets indicated. Error bars are the mean ± SD of four of five mice.

tion that thrombin activates proMMP-9 extends the various modes by which thrombin and MMP-9 may interact. Thrombin has been shown to activate proMMP-2 (Nguyen et al., 2000; Lafleur et al., 2001), but a similar demonstration for proMMP-9 has not been shown to our knowledge.

It is important to note that Tang et al. (2004) have subjected MMP-9 null mice to ICH injury caused by bacterial collagenase, and they report that the null mice had increased mortality, hemorrhage, and brain edema compared with wild type. This result is at odds with that of the current report. A contributing factor could be the nature of the injury used, and this is supported by a recent report (Tejima et al., 2006) that blood-induced ICH caused less edema in the brain of MMP-9 null mice compared with wild type. Besides the difference in models, Tang et al. (2004) used older mice that were 20–35 weeks of age, and it is possible that in aged mice, the long-term loss of MMP-9 activity is compensated by the upregulation of other MMPs, as the authors discussed.

The recognition of thrombin as a mediator of acute neurotoxicity in ICH complicates the treatment of this condition. Thrombin is essential for the formation of a blood clot, and thus its activity is vital to prevent additional enlargement of a hematoma. The aforementioned activated Factor VIIa (Mayer et al., 2005) reduces the size of hematoma after ICH, at least in part by generating thrombin downstream. Thus, the use of activated Factor VIIa could enhance neurotoxicity as suggested by our results. This complexity emphasizes the need to dissect the mechanisms of thrombin neurotoxicity, such that the undesirable mechanisms could be inhibited while sparing the therapeutic blood-clotting functions of thrombin in ICH. In this regard, the use of agents to inhibit PAR-1 and MMP activity, when activated Factor VIIa or thrombin is administered, would seem logical.

The normal CNS contains some basally expressed MMP members, but most are not found in the uninjured state. However, after all types of neural injuries, multiple MMP members are upregulated (Power et al., 2003; Weaver et al., 2005; Wells et al., 2005). The sudden increase in several MMP members is detrimental because they mediate actions that include neurotoxicity, demyelination, and blood–brain barrier leakage (Yong et al., 2001). Although we have focused on MMP-9 here, other MMPs upregulated in ICH, such as MMP-12 (Wells et al., 2005), are likely also capable of mediating neurotoxicity. The inhibition of MMP activity is a viable therapeutic option to alleviate the death of neurons that occur in ICH. Such a treatment, to be initiated soon after injury and for the first few days when MMP expression is high, should not be prolonged because MMPs also have useful functions in subsequent attempts to repair the nervous system (Larsen et al., 2003; Cunningham et al., 2005; Yong, 2005). Indeed, Zhao et al. (2006) reported that the inhibition of MMPs 7 d after stroke injury in rats impaired functional recovery, in contrast to their previous work of the utility of inhibiting MMPs 1 d after injury.

In summary, our results demonstrate that thrombin and MMP-9 have individual and additive effects on neuronal death, *in vitro* and after ICH, *in vivo* (supplemental Fig. 3, available at www.jneurosci.org as supplemental material). To improve the prognosis of ICH, the neurotoxic actions of thrombin and MMPs must be inhibited early and simultaneously after ICH injury.

References

Abilleira S, Montaner J, Molina CA, Monasterio J, Castillo J, Alvarez-Sabin J (2003) Matrix metalloproteinase-9 concentration after spontaneous intracerebral hemorrhage. J Neurosurg 99:65–70.

Ahn HS, Foster C, Boykow G, Stamford A, Manna M, Graziano M (2000) Inhibition of cellular action of thrombin by N3-cyclopropyl-7-[[4-(1-methylethyl)phenyl]methyl]-7H-pyrrolo[3,2-f]quinazoline-1,3-diamine (SCH 79797), a nonpeptide thrombin receptor antagonist. Biochem Pharmacol 60:1425–1434.

Aronowski J, Hall CE (2005) New horizons for primary intracerebral hemorrhage treatment: experience from preclinical studies. Neurol Res 27:268–279.

Berne RM, Levy MN (1998) Blood and hemostasis. In: Physiology, Ed 4 (Berne RM, Levy MN, Koeppen BN, Stanton BA, eds), p 1232. St. Louis: Mosby.

Castellanos M, Leira R, Serena J, Pumar JM, Lizasoain I, Castillo J, Davalos A (2003) Plasma metalloproteinase-9 concentration predicts hemorrhagic transformation in acute ischemic stroke. Stroke 34:40–46.

Citron BA, Zhang SX, Smirnova IV, Festoff BW (1997) Apoptotic, injury-induced cell death in cultured mouse murine motor neurons. Neurosci Lett 230:25–28.

Cocks TM, Moffatt JD (2000) Protease-activated receptors: sentries for inflammation? Trends Pharmacol Sci 21:103–108.

Colman RW, Hirsh J, Marder VJ, Salzman EW (1994) Hemostasis and thrombosis. In: Basic principles and clinical practice. Philadelphia: Lippincott.

Cunningham LA, Wetzel M, Rosenberg GA (2005) Multiple roles for MMPs and TIMPs in cerebral ischemia. Glia 50:329–339.

Figueroa BE, Keep RF, Betz AL, Hoff JT (1998) Plasminogen activators potentiate thrombin-induced brain injury. Stroke 29:1202–1207.

Gu Z, Kaul M, Yan B, Kridel SJ, Cui J, Strongin A, Smith JW, Liddington RC, Lipton SA (2002) S-nitrosylation of matrix metalloproteinases: signaling pathway to neuronal cell death. Science 297:1186–1190.

Hanisch UK, van Rossum D, Xie Y, Gast K, Misselwitz R, Auriola S, Goldsteins G, Koistinaho J, Kettenmann H, Moller T (2004) The microglia-activating potential of thrombin: the protease is not involved in the induction of proinflammatory cytokines and chemokines. J Biol Chem 279:51880–51887.

Kawabata A, Saifeddine M, Al-Ani B, Leblond L, Hollenberg MD (1999) Evaluation of proteinase-activated receptor-1 (PAR1) agonists and antagonists using a cultured cell receptor desensitization assay: activation of PAR2 by PAR1-targeted ligands. J Pharmacol Exp Ther 288:358–370.

Lafleur MA, Hollenberg MD, Atkinson SJ, Knauper V, Murphy G, Edwards DR (2001) Activation of pro-(matrix metalloproteinase-2) (pro-MMP-2) by thrombin is membrane-type-MMP-dependent in human umbilical vein endothelial cells and generates a distinct 63 kDa active species. Biochem J 357:107–115.

Lapchak PA, Chapman DF, Zivin JA (2000) Metalloproteinase inhibition reduces thrombolytic (tissue plasminogen activator)-induced hemorrhage after thromboembolic stroke. Stroke 31:3034–3040.

Larsen PH, Wells J, Stallcup WB, Opdenakker G, Yong VW (2003) Matrix metalloproteinase-9 (MMP-9) facilitates remyelination by processing the inhibitory NG2 proteoglycan. J Neurosci 23:11127–11135.

Lee KR, Colon GP, Betz AL, Keep RF, Kim S, Hoff JT (1996) Edema from intracerebral hemorrhage: the role of thrombin. J Neurosurg 84:91–96.

Lee KR, Kawai N, Kim S, Sagher O, Hoff JT (1997) Mechanisms of edema formation after intracerebral hemorrhage: effects of thrombin on cerebral blood flow, blood-brain barrier permeability, and cell survival in a rat model. J Neurosurg 86:272–278.

Liu WH, Chen XM, Fu B (2000) Thrombin stimulates MMP-9 mRNA expression through AP-1 pathway in human mesangial cells. Acta Pharmacol Sin 21:641–645.

Mayer SA, Brun NC, Begtrup K, Broderick J, Davis S, Diringer MN, Skolnick BE, Steiner T, Recombinant Activated Factor VII Intracerebral Hemorrhage Trial Investigators (2005) Recombinant activated factor VII for acute intracerebral hemorrhage. N Engl J Med 352:777–785.

Mendelow AD (1993) Mechanisms of ischemic brain damage with intracerebral hemorrhage. Stroke 24 I115–I117.

Montaner J, Molina CA, Monasterio J, Abilleira S, Arenillas JF, Ribo M, Quintana M, Alvarez-Sabin J (2003) Matrix metalloproteinase-9 pretreatment level predicts intracranial hemorrhagic complications after thrombolysis in human stroke. Circulation 107:598–603.

Nguyen M, Arkell J, Jackson CJ (2000) Three-dimensional collagen matrices induce delayed but sustained activation of gelatinase A in human endothelial cells via MT1-MMP. Int J Biochem Cell Biol 32:621–631.

Oh LYS, Larsen PH, Krekoski CA, Edwards DR, Donovan F, Werb Z, Yong VW (1999) Matrix metalloproteinase-9/gelatinase B is required for process outgrowth by oligodendrocytes. J Neurosci 19:8464–8475.

Opdenakker G, Van den Steen PE, Dubois B, Nelissen I, Van Coillie E, Masure S, Proost P, Van Damme J (2001) Gelatinase B functions as regulator and effector in leukocyte biology. J Leukoc Biol 69:851–859.

Power C, Henry S, Del Bigio MR, Larsen PH, Corbett D, Imai Y, Yong VW, Peeling J (2003) Intracerebral hemorrhage induces macrophage activation and matrix metalloproteinases. Ann Neurol 53:731–742.

Qureshi AI, Tuhrim S, Broderick JP, Batjer HH, Hondo H, Hanley DF (2001) Spontaneous intracerebral hemorrhage. N Engl J Med 344:1450–1460.

Rosell A, Ortega-Aznar A, Alvarez-Sabin J, Fernandez-Cadenas I, Ribo M, Molina CA, Lo EH, Montaner J (2006) Increased brain expression of matrix metalloproteinase-9 after ischemic and hemorrhagic human stroke. Stroke 37:1399–1406.

Rosenberg GA (2002) Matrix metalloproteinases in neuroinflammation. Glia 39:279–291.

Rosenberg GA, Navratil M (1997) Metalloproteinase inhibition blocks edema in intracerebral hemorrhage in the rat. Neurology 48:921–926.

Rosenberg GA, Estrada EY, Dencoff JE (1998) Matrix metalloproteinases and TIMPs are associated with blood-brain barrier opening after reperfusion in rat brain. Stroke 29:2189–2195.

Schmued LC, Albertson C, Slikker Jr W (1997) Fluoro-Jade: a novel fluorochrome for the sensitive and reliable histochemical localization of neuronal degeneration. Brain Res 751:37–46.

Stephenson CD, Lockwood CJ, Ma Y, Guller S (2005) Thrombin-dependent regulation of matrix metalloproteinase (MMP)-9 levels in human fetal membranes. J Matern Fetal Neonatal Med 18:17–22.

Striggow F, Riek M, Breder J, Henrich-Noack P, Reymann KG, Reiser G (2000) The protease thrombin is an endogenous mediator of hippocampal neuroprotection against ischemia at low concentrations but causes degeneration at high concentrations Proc Natl Acad Sci USA 97:2264–2269.

Tang J, Liu J, Zhou C, Alexander JS, Nanda A, Granger DN, Zhang JH (2004) MMP-9 deficiency enhances collagenase-induced intracerebral hemorrhage and brain injury in mutant mice. J Cereb Blood Flow Metab 24:1133–1145.

Tejima E, Zhao BQ, Tsuji K, Rosell A, van Leyen K, Gonzalez RG, Montaner J, Wang X, Lo EH (2006) Astrocytic induction of matrix metalloproteinase-9 and edema in brain hemorrhage. J Cereb Blood Flow Metab, in press.

Vecil GG, Larsen PH, Corley SM, Herx LM, Besson A, Goodyer CG, Yong VW (2000) Interleukin-1 is a key regulator of matrix metalloproteinase-9 expression in human neurons in culture and following mouse brain trauma in vivo. J Neurosci Res 61:212–224.

Vu TH, Shipley JM, Bergers G, Berger JE, Helms JA, Hanahan D, Shapiro SD, Senior RM, Werb Z (1998) MMP-9/gelatinase B is a key regulator of growth plate angiogenesis and apoptosis of hypertrophic chondrocytes. Cell 93:411–422.

Wang J, Tsirka SE (2005) Neuroprotection by inhibition of matrix metalloproteinases in a mouse model of intracerebral haemorrhage. Brain 128:1622–1633.

Wang X, Lo EH (2003) Triggers and mediators of hemorrhagic transformation in cerebral ischemia. Mol Neurobiol 28:229–244.

Weaver A, Goncalves da Silva A, Nuttall RK, Edwards DR, Shapiro SD, Rivest S, Yong VW (2005) An elevated matrix metalloproteinase in experimental autoimmune encephalomyelitis is protective by affecting Th1/Th2 polarization. FASEB J 19:1668–1670.

Weinstein JR, Hong S, Kulman JD, Bishop C, Kuniyoshi J, Andersen H, Ransom BR, Hanisch UK, Moller T (2005) Unraveling thrombin's true microglia-activating potential: markedly disparate profiles of pharmaceutical-grade and commercial-grade thrombin preparations. J Neurochem 95:1177–1187.

Wells JE, Rice TK, Nuttall RK, Edwards DR, Zekki H, Rivest S, Yong VW (2003) An adverse role for matrix metalloproteinase 12 after spinal cord injury in mice. J Neurosci 23:10107–10115.

Wells JE, Biernaskie J, Szymanska A, Larsen PH, Yong VW, Corbett D (2005) Matrix metalloproteinase (MMP)-12 expression has a negative impact on sensorimotor function following intracerebral haemorrhage in mice. Eur J Neurosci 21:187–196.

Xi G, Keep RF, Hoff JT (2006) Mechanisms of brain injury after intracerebral haemorrhage. Lancet Neurol 5:53–63.

Xue M, Del Bigio MR (2000) Intracerebral injection of autologous whole blood in rats: time course of inflammation and cell death. Neurosci Lett 283:230–232.

Xue M, Del Bigio MR (2001) Acute tissue damage after injections of thrombin and plasmin into rat striatum. Stroke 32:2164–2169.

Xue M, Del Bigio MR (2003) Comparison of brain cell death and inflammatory reaction in three models of intracerebral hemorrhage in adult rats. J Stroke Cerebrovasc Dis 12:152–159.

Xue M, Del Bigio MR (2005) Injections of blood, thrombin, and plasminogen more severely damage neonatal mouse brain than mature mouse brain. Brain Pathol 15:273–280.

Yong VW (2005) Metalloproteinases: mediators of pathology and regeneration in the CNS. Nat Rev Neurosci 6:931–944.

Yong VW, Power C, Forsyth P, Edwards DR (2001) Metalloproteinases in biology and pathology of the nervous system. Nat Rev Neurosci 2:502–511.

Yoshida S, Shiosaka S (1999) Plasticity-related serine proteases in the brain. Int J Mol Med 3:405–409.

Zhao BQ, Wang S, Kim HY, Storrie H, Rosen BR, Mooney DJ, Wang X, Lo EH (2006) Role of matrix metalloproteinases in delayed cortical responses after stroke. Nat Med 12:441–445.